



## Lateral manipulation and interplay of local Kondo resonances in a two-impurity Kondo system

Jindong Ren, Xu Wu, Haiming Guo, Jinbo Pan, Shixuan Du, Hong-Gang Luo, and Hong-Jun Gao

Citation: [Applied Physics Letters](#) **107**, 071604 (2015); doi: 10.1063/1.4929327

View online: <http://dx.doi.org/10.1063/1.4929327>

View Table of Contents: <http://scitation.aip.org/content/aip/journal/apl/107/7?ver=pdfcov>

Published by the [AIP Publishing](#)

---

### Articles you may be interested in

[Understanding the Kondo resonance in the d-CoPc/Au\(111\) adsorption system](#)

J. Chem. Phys. **141**, 084713 (2014); 10.1063/1.4893953

[Local thickness determination of thin insulator films via localized states](#)

Appl. Phys. Lett. **104**, 231606 (2014); 10.1063/1.4883219

[Effects of tip induced carrier density in local tunnel spectra of graphene](#)

Appl. Phys. Lett. **98**, 102109 (2011); 10.1063/1.3555344

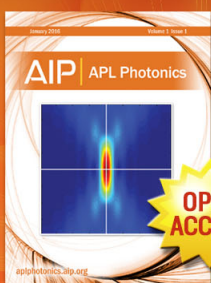
[Coulomb staircases by lateral tunneling between adjacent nanoclusters formed on Si surfaces](#)

J. Vac. Sci. Technol. B **18**, 2365 (2000); 10.1116/1.1290367

[Single-electron tunneling study of two-dimensional gold clusters](#)

Appl. Phys. Lett. **77**, 1179 (2000); 10.1063/1.1289500

---



Launching in 2016!  
The future of applied photonics research is here

AIP | APL  
Photonics

## Lateral manipulation and interplay of local Kondo resonances in a two-impurity Kondo system

Jindong Ren,<sup>1</sup> Xu Wu,<sup>1</sup> Haiming Guo,<sup>1,a)</sup> Jinbo Pan,<sup>1</sup> Shixuan Du,<sup>1</sup> Hong-Gang Luo,<sup>2,3</sup> and Hong-Jun Gao<sup>1</sup>

<sup>1</sup>*Institute of Physics, Chinese Academy of Sciences, Beijing 100190, China*

<sup>2</sup>*Center for Interdisciplinary Studies and Key Laboratory for Magnetism and Magnetic Materials of the MoE, Lanzhou University, Lanzhou 730000, China*

<sup>3</sup>*Beijing Computational Science Research Center, Beijing 100084, China*

(Received 15 June 2015; accepted 10 August 2015; published online 20 August 2015)

The atomic-scale spatial relationship of a two-impurity Kondo system has been determined at varying lateral distance by scanning tunneling microscopy (STM) and spectroscopy. The localized spins of two cobalt magnetic adatoms that are placed on different electrodes of an STM form two individual Kondo singlet states, each showing quite different Kondo coupling, i.e., the tip-Kondo with low Kondo temperature and the sample-Kondo with high Kondo temperature. The differential conductance  $dI/dV$  spectra show the continuous changes of the resonance peak feature when approaching the Kondo tip laterally to the local sample-Kondo impurity on the surface. The result indicates a notable interplay between these two Kondo systems. We propose a convolution model based on the  $q$  factor of the sample-Kondo ( $q_s$ ) and tip-Kondo ( $q_t$ ) to interpret the change of various tunneling channels and the evolution of the experimental spectra. © 2015 AIP Publishing LLC.

[<http://dx.doi.org/10.1063/1.4929327>]

Investigation of the Kondo-screened system<sup>1</sup> is of great importance for the development of nanoscale spintronic devices based on atomic-size junctions. Coupling between a localized spin and the surrounding conduction electrons will lead to anomalous transport measurements and cause a narrow electronic resonance in the local density of states (LDOS) around the Fermi energy below the Kondo temperature ( $T_K$ ). Scanning tunneling microscopy and spectroscopy (STM/STS) have been applied to detect the Kondo resonance for individual magnetic atoms on different metal substrates.<sup>2,3</sup> For a traditional investigation, a spectroscopically featureless STM tip was used locally to probe the single magnetic impurity system.<sup>4,5</sup> From these experiments, the Kondo physics has been well defined, and a so-called Fano line shape can be observed in the conductance characteristics. Within the Fano theory, the line shape parameter  $q$  describes the ratio of the probabilities between the indirect electrons tunneling via the magnetic impurity and the direct tunneling into the metal host.<sup>6</sup>

If changing the traditional STM tip into a Kondo tip, rich physics involving a two-impurity Kondo system (2IKS)<sup>7,8</sup> will arise. Recently, Bork *et al.* identified two different coupling regimes and observed the quantum phase transition by approaching vertically a Co-terminated gold tip toward another Co adatom on Au(111) surface.<sup>9</sup> A splitting feature was found in  $dI/dV$  spectra when the two Co impurities keep extreme low separations in a point-contact regime. However, studying the electronic transport mechanism<sup>10</sup> in the 2IKS is more crucial and general when each impurity stays in its own Kondo singlet states, for example, for the transport properties in quantum dot devices.<sup>11</sup> In this regime, the two tunneling channels in a one-impurity Kondo system will increase to four channels, and the quantum interference

becomes much more complex if the two magnetic impurities are manipulated laterally. The changes in the tunneling paths<sup>6,12</sup> will affect the interplay of the two Kondo singlet states, yielding different  $dI/dV$  line shapes, especially for two totally different Kondo singlet states. It is not clear how the resonance spectrum evolves with the interplay of two impurity Kondo systems when the tunneling channels vary at different lateral distances.<sup>13</sup>

In this letter, we demonstrate the investigation of lateral movement of a local Kondo resonance probed with a Kondo tip by a precise control in an STM experiment. After attaching one Co adatom to the featureless STM tip, a Kondo tip system is fabricated with a very low  $T_K$  ( $\sim 1.6$  K). While the Co adatoms on the Ru(0001) substrate constitute a sample Kondo system showing a high  $T_K$  ( $\sim 200$  K).<sup>14</sup> The  $dI/dV$  spectra show the continuous changes of the resonance peak feature when approaching the Kondo tip laterally close to the sample-Kondo impurity. The result indicates a notable interplay between these two Kondo singlet states. A simple convolution model based on the  $q$  factor of the sample-Kondo ( $q_s$ ) and tip-Kondo ( $q_t$ ) was introduced to interpret the evolution of the experimental  $dI/dV$  spectra. In this model, the tunneling channels in 2IKS will be altered with the lateral manipulation of the two local Kondo resonances<sup>6</sup> leading to the unique spectral features.

The experiments were performed in an ultrahigh vacuum low temperature STM (LT-STM) system (Unisoku) operating at  $T = 0.45$  K with magnetic field perpendicular to the surface. The Ru(0001) crystal was prepared by repeated cycles of sputtering and annealing. Cobalt was deposited *in situ* at  $\sim 20$  K from a Co rod (purity of 99.99%) using a commercial electron beam evaporator. Tip states were calibrated on bare Ru(0001) before and after measurements to ensure that there are no tip-related features in the recorded  $dI/dV$  spectra.

Figure 1(a) displays an STM topographic image of individual Co adatoms deposited on Ru(0001) surface. All the

<sup>a)</sup>E-mail: hmguo@iphy.ac.cn

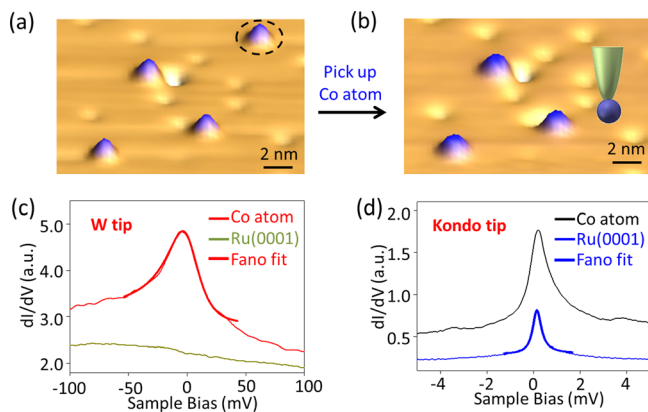


FIG. 1. Fabrication of the two-impurity Kondo system. (a) and (b) Topography of the picking up process: the Co adatom labeled in the black dashed ellipse was attached to the STM tip by applying a voltage pulse. (c) Spectroscopic measurements taken on Co atom (the red thin line) and bare Ru(0001) surface (the olive thin line) with a spectroscopically featureless STM tip. The red thick line is the Fano fit result. (d) Spectroscopic measurements taken on a Co adatom (the black thin line) and bare Ru(0001) surface (the blue thin line) with a Co-terminated STM tip. The blue thick line is the Fano fit result. All STS were performed at  $T = 0.45$  K.

adatoms have the same full width at half maximum (FWHM) of  $\sim 10$  Å with a tunneling resistance of  $2$  G $\Omega$ . A nonmagnetic tungsten tip was used to detect the  $dI/dV$  spectra of Co adatoms and of bare Ru(0001) surface, see Fig. 1(c). The STS spectrum of Ru(0001) is featureless in the range of  $\pm 100$  mV, while it shows a broad but asymmetric lineshape peak of Co adatoms around Fermi energy. This broad peak can be attributed to a Kondo resonance since the theoretically calculated magnetic moment of Co on Ru(0001) is nearly  $1 \mu_B$ .<sup>15</sup> By fitting the Kondo peak with the Fano-Lorentz function,<sup>16</sup> we obtain a  $T_K$  of  $\sim 200$  K and  $q$  factor of 3.8. The Kondo feature is quite different from that of Co adatom on Au(111) with  $T_K = \sim 70$  K and  $q < 1$ ,<sup>6,13</sup> in which it shows a narrower, asymmetric dip. The higher  $T_K$  here manifests a strong coupling strength between the Co adatoms and the Ru substrate according to the proportional relationship.<sup>17</sup>

A Co-terminated STM tip is used to create a tip-Kondo system. To attach single cobalt atoms to the STM tip, we position the tip on top of an adatom and apply a voltage pulse<sup>18,19</sup> (Fig. 1(a)), e.g.,  $+4.0$  V for  $0.2$  s with feedback loop off. After a successful pulse, the target Co adatom disappears from the surface (Fig. 1(b)). The subsequent  $dI/dV$  measurements on the clean Ru(0001) surface (Fig. 1(d)) manifest a sharp narrow peak around Fermi energy. Hence, both the STM image and spectrum certify that the Co adatom was attached to the tip apex. Magnetic field dependent measurements were carried out to prove that the observed sharp peak is truly caused by a tip-Kondo resonance. As shown in Fig. 2, the peak shows Zeeman splitting as a function of the magnetic field, consistent well with spin  $1/2$  Kondo physics.<sup>6</sup> The splitting energy is linearly related to the external magnetic field. By fitting the energy to the formula  $\Delta = g\mu_B B$ , we obtain a  $g$  factor of about  $1.88 \pm 0.02$  (Fig. 2(b)).<sup>20</sup>

We then fit the peak of the tip-Kondo system with a Fano-Lorentz function (Fig. 1(d)). From the FWHM of the peak,  $T_K$  can be extracted as  $1.57 \pm 0.04$  K after correction for measured temperature and modulation broadening. The

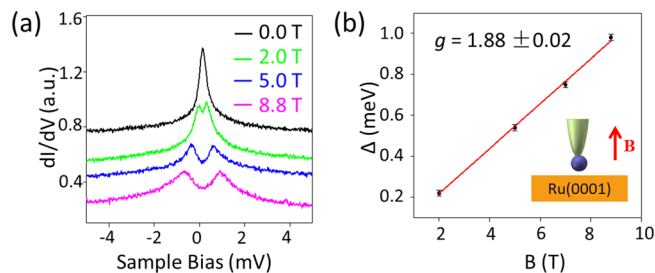


FIG. 2. (a) The Kondo peaks of the tip Kondo system are split under different magnetic fields. Spectra for labels 0.0 T, 2.0 T, 5.0 T, and 8.8 T have been shifted vertically by 0.55, 0.33, 0.19, and  $-0.03$ , respectively. (b) Magnetic field dependent of the Zeeman energy with  $g$  factor of  $1.88 \pm 0.02$ . Error bars represent standard deviations achieved in the fitting process. The inset shows a schematic diagram of STS taken on bare Ru surface with a Co-terminated tip under perpendicular magnetic fields.

$q$  factor is fitted as 22.8. The curve can be also fitted with Doniach-Sunjic function and a  $T_K$  of  $0.92 \pm 0.03$  K is thus obtained. With both these fitting methods, the extremely low Kondo temperature of tip Kondo system can be clearly established. This indicates a very weak coupling strength between Co adatom and its surrounding itinerant electrons. Although the precise environment of the Co adatom on the tip cannot be controlled and identified well, the tip Kondo feature with low  $T_K$  can be reproduced. The high  $q$  factor demonstrates that the electron tunneling through the magnetic Co tip apex is absolutely dominant compared to that through the bare tungsten area in the tip.

As a consequence, two quite different Kondo systems were created, i.e., the tip-Kondo with low  $T_K$  and the sample-Kondo with high  $T_K$ . Each of them forms one individual Kondo singlet state. Then we move the Kondo tip close to the center of the Co adatom at the Ru surface ( $Co_s$ ), just as illustrated in Fig. 3. During the movement, the tunneling parameters are set as  $I = -0.2$  nA,  $V_b = -0.02$  V. Figure 3(b) reveals the observed experimental  $dI/dV$  data as a function of the separation between the two Co adatoms. The measured  $dI/dV$  curve begins to change when the tip is about  $0.7$  nm away from the center of the Co adatom. The resonance peak becomes broader slightly and continuously, while its intensity decreases first and afterwards increases, leading to a minimum peak intensity at about  $3.5$  Å in a series of data. Moreover, the peak seems a little asymmetric when it's very close to the

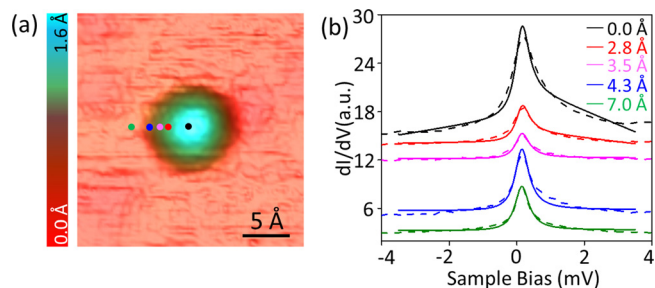


FIG. 3. (a), STM topography of single Co adatom on Ru(0001) surface; (b), Lateral dependence of Kondo resonance line shapes taken closer to the center of Co adatom (see (a)) with a Kondo tip (the Co adatom is attached on the tip apex). The dashed lines display the measured spectra, and the solid lines are the fitted results using method described in the manuscript. Spectra for labels 0.0 Å, 2.8 Å, 3.5 Å, 4.3 Å, and 7.0 Å have been shifted vertically by 12.1, 12.9, 11.2, 3.1, and 0.6, respectively,  $T = 0.45$  K, tunneling parameters:  $I = -0.2$  nA,  $V_b = -0.02$  V.

center. Chen *et al.* reported the approaching of two Co adatom that both sited on the Au(111) surface.<sup>13</sup> The strong interplay of the two Co adatom will quench the Kondo signal when the distance is rather small. While in our case, the vertical distance determined by the tunneling junction makes the Co adatoms always in their own Kondo singlet.

Based on the individual Kondo singlet state of the tip-Kondo and the sample-Kondo, in the following, we discuss the interplay between these two states to understand the observed data. For a single-impurity Kondo system detected with featureless tip, the tunneling current originates from the interference between the direct tunneling into the host ( $t_2'$ ) and the indirect tunneling via the magnetic adatom ( $t_1'$ ).<sup>6</sup> The shape of the resonance in the  $dI/dV$  spectra depends strongly on the weight of these two tunneling channels. To analyze the experimental data quantitatively, a Fano equation was introduced to describe the line shape as

$$\frac{dI}{dV} \propto \frac{(q + \tilde{\varepsilon})^2}{1 + \tilde{\varepsilon}^2}. \quad (1)$$

Here,  $\tilde{\varepsilon} = \frac{\omega - \varepsilon_K}{\Gamma}$ ,  $\omega = eV$ ,  $q$  is the interference parameter that controls the line shape of the Fano function. Actually, the tunneling matrix elements  $t_2'$  and  $t_1'$  are involved in the  $q$  factor as  $q \propto t_1'/t_2'$ . The lineshape will manifest a Lorentzian peak when the indirect channel acts as the primary contributor.

For our measurements on the two-impurity Kondo system, the tip-sample separation is still large at a tunneling resistance of 2 G $\Omega$ ;<sup>21</sup> thus, one cannot observe the splitting behavior as obtained in Bork's paper.<sup>9</sup> We believe that the two Co atoms at different electrodes interact weakly and stay in their own Kondo states. The tip will be used only as a local detector and will not affect the underlying Kondo singlet state. For each individual system, the LDOS can be expressed as the following Fano equations:

$$\rho_s \propto \frac{(q_s + \tilde{\varepsilon}_s)^2}{1 + \tilde{\varepsilon}_s^2}, \quad (2)$$

$$\rho_t \propto \frac{(q_t + \tilde{\varepsilon}_t)^2}{1 + \tilde{\varepsilon}_t^2}. \quad (3)$$

To explain the observed  $dI/dV$  spectrum, we start with the quantum mechanics in the STM tunneling equation and calculate the convolution of the tunneling channels in the tip and sample-Kondo systems. The  $dI/dV$  spectrum can be expressed by

$$\frac{dI}{dV} \propto \rho_t(-eV)\rho_s(0) + \int_0^{eV} \frac{d}{dE} \rho_s(E)\rho_t(E - eV)dE, \quad (4)$$

where  $V$  is the bias voltage,  $\rho_t$  and  $\rho_s$  are the LDOS of the tip and sample, respectively.

Using Equations (2)–(4), we fit the experimental  $dI/dV$  data by the convolution of the sample-Kondo ( $q_s$ ) and tip-Kondo ( $q_t$ ) systems. The fitted curves are displayed by the solid lines in Fig. 3(b). Figure 4(d) indicates the evolution of the  $q_s$  and  $q_t$  factors for the two systems as function of the tip-sample lateral distance, which have opposite trends.

To further understand the evolution of the  $q_s$  and  $q_t$  factors, and their physical meaning for the tip-Kondo and

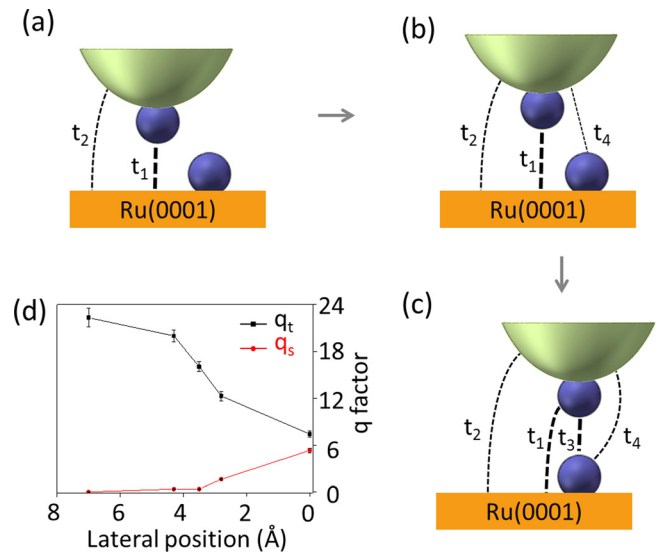


FIG. 4. (a)–(c), schematic diagrams of tunneling channel changes during the lateral movement of Kondo tip relative to a Co adatom on Ru(0001) surface; (d), the evolution of the two  $q$  factors for the tip-Kondo peak ( $q_t$ ) and the sample-Kondo peak ( $q_s$ ) as functions of the lateral distances between the two Co impurities. Error bars represent standard deviations achieved in the fitting process.

sample-Kondo system, we turn to the constituted tunneling matrices  $t$ . Just as motioned above, the  $q$  factor relies strongly on the ratio of tunneling currents between the direct and indirect tunneling channels. In the two-impurity Kondo system, electrons emitted from the probing tip now have four paths to tunnel into the sample side. The tunneling channels labeled as  $t_1$ – $t_4$  are defined in Fig. 4(c). The previous tunneling path ( $t_1'$  or  $t_2'$ ) in the Kondo system detected by normal tip here can be divided into two segments for each electrode. We can give the relations between the  $q_s$  and  $q_t$  factors and the tunneling matrices as follows:

$$q_s \propto \frac{t_3 + t_4}{t_1 + t_2}, \quad (5)$$

$$q_t \propto \frac{t_1 + t_3}{t_2 + t_4}. \quad (6)$$

During the fitting process, we actually hypothesized that the widths ( $\Gamma$ ) and positions ( $\varepsilon_K$ ) of both the tip and sample Kondo resonances are constant, and the evolution of the  $dI/dV$  spectra arise only from the weight variations of the tunneling matrices in each channel, which are reflected by the changes of  $q_s$  and  $q_t$  factors.

In our experiment, the Kondo tip is placed far away (more than  $\sim 7.0$  Å in Fig. 4(d)) from the Co<sub>s</sub> adatom at the beginning of the manipulation experiment. A symmetric peak caused by the one-impurity tip-Kondo case is easily observed. The tunneling current originates from channels  $t_1$  and  $t_2$ . The excess electrons into the tip electrode will come mainly from the  $t_1$  channel rather than from  $t_2$ , and  $q_t$  is equal to the initial value of 22.8.

While moving the tip closer (less than  $\sim 7.0$  Å, see Figs. 4(a) and 4(b)) to the Co<sub>s</sub>, the  $dI/dV$  peak intensity will decrease. The fitted results show that a near-zero  $q_s$  will arise while the  $q_t$  deviates from the one impurity tip Kondo case. This can be understood from the involved tunneling matrix

elements. When the Kondo tip apex is close to the Co<sub>s</sub> adatom, the direct current through the Co<sub>s</sub> (channel  $t_4$ ) that contributes to the  $q_s$  will first appear while the tunneling contribution in  $t_1$  and  $t_2$  will decrease. Due to the large  $q_t$  value, the electron current in channel  $t_4$  is rather small at this stage. The gradual enhancement of  $t_4$  and  $q_s$  demonstrates that the sample-Kondo system has participated in the 2IKS system. It will also lead to the decline in  $q_t$  from the one-impurity tip-Kondo case and cause the decrease of the peak intensity in the  $dI/dV$  spectra.

By moving the Kondo tip closer to the Co<sub>s</sub> (see Figs. 4(b) and 4(c)), the intensity of the peak in  $dI/dV$  spectra will turn to increase and leave a minimum at a lateral distance of about 3.5 Å (Fig. 3(b)). Moreover, the shape of the peak becomes apparently more asymmetric. From the fitted  $q$  values in Fig. 4(d), we can find a tendency for the  $q_s$  to increase rapidly, as well as a fast falling  $q_t$ . At this stage, the weak coupling between the  $d$  orbitals of the two magnetic impurities in the tunneling region will open an extra tunneling channel ( $t_3$ ). It will further promote the Co<sub>s</sub> impact and alter the distribution of the tunneling matrix elements. During the movement, both the tunneling channels  $t_3$  and  $t_4$  will increase while the  $t_1$  and  $t_2$  channels will decrease at different rates. Therefore, the magnitude of the  $q_s$  will increase continuously<sup>22</sup> according to Equation (5). Indeed, the rapid increase of the  $q_s$  in Fig. 4(d) indicates that the existence of the Co<sub>s</sub> will give rise to a more remarkable contribution. Comparing to the bare Ru surface, the existence of a Co magnetic impurity improves the localized states under the tip and enhances the peak intensity.<sup>23</sup> This behavior is similar to the spatial dependence of the Kondo resonance of Co adatom on other surfaces, in which the intensity of the Kondo peak decreases monotonically at the position away from the center of Co adatom.<sup>14</sup> Furthermore, the upper limit of the influence radius of the magnetic impurity on the LDOS of surface is less than 10 Å, and the significant influence occurs usually within an area of 0.35 nm diameter around the magnetic impurity.<sup>3</sup> The result is consistent with the experiment of Chen *et al.*<sup>13</sup> as well, in which the Kondo spectra measured on Co atoms did not deviate significantly until the inter-cobalt separations decreases to 6 Å.

Finally, we discuss the situation that the Co-terminated tip is positioned on top of Co<sub>s</sub> adatom (see Fig. 4(c)). The apparent  $T_K$  is extracted as  $4.82 \pm 0.04$  K from the width of the peak after correction for measured temperature and modulation broadening. The width and intensity of the peak seems to be much more influenced by the tip-Kondo system than by the sample-Kondo system, in which the former has a far lower  $T_K$  than the latter. However, the peak has an asymmetric line shape, similar to the sample-Kondo system. It can be explained by the fitted values of  $q_s$  and  $q_t$  factors (5.5 and 7.3, respectively), which are closer to the initial  $q$  factor (3.8) of the sample-Kondo system than that (22.8) of the tip-Kondo system. This result indicates that although the electron tunneling channels through the magnetic impurities are dominant paths compared to that through the metal hosts, the Co adatom at the substrate plays a more important role for the selection of the electron tunneling paths than the Co-terminated Kondo tip.

In summary, we experimentally manipulate and probe a lateral approach of a Kondo impurity by using a Kondo STM

tip. During the movement, the tip-Kondo system plays a dominant role at the beginning, afterward the sample-Kondo system joins and constitutes the 2IKS. The tunneling spectrum is a superposition of the Kondo resonances of both tip and sample. The evolution of the experimental data can be interpreted well by the  $q_s$  and  $q_t$  factors, as well as continuous changing of the weight in each tunneling channel. Our experiment offers a universal way to investigate the space variation of the tunneling matrix elements for the tunneling process in a weakly coupled 2IKS. The constructed 2IKS will provide a way for studying the transport properties of magnetic quantum dot devices and the rich physics in the two-impurity Kondo model.

We thank S. Pantellides at Vanderbilt University and W. Hofer at Newcastle University for helpful discussions. Work in China was supported by National Natural Science Foundation of China (Grant Nos. 51210003, 61274011, 11190024, 11325417, and 11174115), National “973” projects of China (Grant Nos. 2013CBA01600 and 2015CB921303), the Chinese Academy of Sciences, and Shanghai supercomputer center.

- <sup>1</sup>W. J. de Haas, J. de Boer, and G. J. van den Berg, *Physica (Utrecht)* **1**, 1115 (1934).
- <sup>2</sup>J. Li, W. D. Schneider, R. Berndt, and B. Delley, *Phys. Rev. Lett.* **80**, 2893 (1998).
- <sup>3</sup>V. Madhavan, W. Chen, T. Jamneala, M. Crommie, and N. Wingreen, *Science* **280**, 567 (1998).
- <sup>4</sup>L. Limot, J. Kröger, R. Berndt, A. Garcia-Lekue, and W. A. Hofer, *Phys. Rev. Lett.* **94**, 126102 (2005).
- <sup>5</sup>N. Néel, J. Kröger, L. Limot, K. Palotas, W. A. Hofer, and R. Berndt, *Phys. Rev. Lett.* **98**, 016801 (2007).
- <sup>6</sup>M. Ternes, A. J. Heinrich, and W. D. Schneider, *J. Phys.: Condens. Matter* **21**, 053001 (2009).
- <sup>7</sup>P. Wahl, P. Simon, L. Diekhöner, V. S. Stepanyuk, P. Bruno, M. A. Schneider, and K. Kern, *Phys. Rev. Lett.* **98**, 056601 (2007).
- <sup>8</sup>A. M. Chang and J. C. Chen, *Rep. Prog. Phys.* **72**, 096501 (2009).
- <sup>9</sup>J. Bork, Y.-h. Zhang, L. Diekhöner, L. Borda, P. Simon, J. Kroha, P. Wahl, and K. Kern, *Nat. Phys.* **7**, 901 (2011).
- <sup>10</sup>I. J. Hamad, L. Costa Ribeiro, G. B. Martins, and E. V. Anda, *Phys. Rev. B* **87**, 115102 (2013).
- <sup>11</sup>J. J. Parks, A. R. Champagne, G. R. Hutchison, S. Flores-Torres, H. D. Abruña, and D. C. Ralph, *Phys. Rev. Lett.* **99**, 026601 (2007).
- <sup>12</sup>J. Figgins and D. K. Morr, *Phys. Rev. Lett.* **104**, 187202 (2010).
- <sup>13</sup>W. Chen, T. Jamneala, V. Madhavan, and M. F. Crommie, *Phys. Rev. B* **60**, R8529 (1999).
- <sup>14</sup>J. Ren, H. Guo, J. Pan, Y. Y. Zhang, X. Wu, H. G. Luo, S. Du, S. T. Pantelides, and H. J. Gao, *Nano Lett.* **14**, 4011 (2014).
- <sup>15</sup>Density functional theory (DFT) based first principles calculations were performed using the Vienna *ab initio* simulation package (VASP). The projector augmented wave (PAW) potentials were used to describe the core electrons, and the local density approximation (LDA) was used for exchange and correlation. The periodic slab models include a vacuum layer of 15 Å. The energy cutoff of the plane-wave basis sets was 400 eV, and the K-points sampling was  $3 \times 3 \times 1$ .
- <sup>16</sup>U. Fano, *Phys. Rev.* **124**, 1866 (1961).
- <sup>17</sup>H. Prüser, M. Wenderoth, P. E. Dargel, A. Weismann, R. Peters, T. Pruschke, and R. G. Ulbrich, *Nat. Phys.* **7**, 203 (2011).
- <sup>18</sup>D. M. Eigler and E. K. Schweizer, *Nature* **344**, 524 (1990).
- <sup>19</sup>S. W. Hla, *Rep. Prog. Phys.* **77**, 056502 (2014).
- <sup>20</sup>A. J. Heinrich, J. A. Gupta, C. P. Lutz, and D. M. Eigler, *Science* **306**, 466 (2004).
- <sup>21</sup>D. J. Choi, M. V. Rastei, P. Simon, and L. Limot, *Phys. Rev. Lett.* **108**, 266803 (2012).
- <sup>22</sup>N. Knorr, M. A. Schneider, L. Diekhöner, P. Wahl, and K. Kern, *Phys. Rev. Lett.* **88**, 096804 (2002).
- <sup>23</sup>H. Pruser, M. Wenderoth, A. Weismann, and R. G. Ulbrich, *Phys. Rev. Lett.* **108**, 166604 (2012).